Pervaporation of acetone/water mixture by PDMS-PTFE/PVDF composite membrane

Qian-Zhi Zhang[a], Bing-Bing Li[a], Peng-Xian Li[a], Da-Yong Li[b], Ping Yang[a], De Sun[a],*

[a]*Department of Chemical Engineering, Changchun University of Technology, 2055 Yanan Street, Changchun 130012, P.R. China,
Tel. +86 155 4357 4855; email: jixiangwu@126.com (Q.-Z. Zhang), Tel. +86 155 2663 9820; email: 1010716404@qq.com (B.-B. Li),
Tel. +86 159 4807 5219; email: 1500649327@qq.com (P.-X. Li), Tel. +86 132 1430 6948; email: 1017120165@qq.com (P. Yang),
Tel. +86 155 2663 9628; email: sunde2002@126.com (D. Sun)*
[b]*COFCO Bio-Chemical Energy (Yushu) Co., Ltd. Economic Development Wukeshu, 1 Dongfeng Street, Changchun 130033,
P.R. China, Tel. +86 136 1071 7573; email: 1184895780@qq.com*

ABSTRACT

The polytetrafluoroethylene (PTFE) particles filled polydimethylsiloxane (PDMS) composite membranes supported by flat sheet PVDF membrane were prepared for the pervaporation (PV) separation of acetone from water. The dissolution and diffusion behaviors of acetone and water and the PV performances of acetone solution in the PDMS-PTFE/PVDF membranes were studied. With increasing PTFE content from 0 to 40 wt.%, solubility selectivity increased and diffusion selectivity firstly kept stable and then decreased; when PTFE loading was 20 wt.%, the composite membrane showed the best PV performance with acetone flux 169 g/(m^2 h), separation factor (α) 40, and permeate separation index (PSI) 8,015 g/(m^2 h). With feed temperature increased from 30 to 50°C, both solubility selectivity and diffusion selectivity decreased; both acetone flux and water flux increased but separation factor decreased at 20 wt.% PTFE content. With the increase in feed flow rate from 60 to 2,000 mL/h, both separation factor and acetone flux firstly increased sharply then maintained steady. When acetone concentration increased from 0.5 to 30.0 wt.%, acetone flux and separation factor increased; acetone permeance and selectivity decreased; the flux and permeance of water remained constant.

Keywords: Poly (dimethylsiloxane); Polytetrafluoroethylene; Pervaporation; Acetone/Water mixture

1. Introduction

Acetone is colorless, flammable, and soluble in water. It is widely used in the production of plastics, explosives, and chemicals and is a very important solvent in pharmaceutical industry [1]. It is also used as a demulsifier to turn stable seawater-in-petroleum emulsions into reusable oil and clean aqueous phase [2]. In one hand, the main traditional acetone production is isopropyl benzene method, which is tedious and causes environmental pollution. In another hand, acetone wastewater generated in a number of industrial processes can cause pollution to the environment. So it is necessary to retrieve acetone from acetone–butanol–ethanol (ABE) broth processes or wastewater

*Corresponding author.

stream which contains acetone. There have been lots of methods (including distillation [3], adsorption [4–6], gas stripping [7,8], liquid–liquid extraction [9], membrane distillation [10], thermopervaporation [11,12], and pervaporation [13–15]) to retrieve acetone. Among these methods, pervaporation is considered as a better separation technology for high efficiency and energy saving.

Pervaporation (PV) is a separation process in which one or more components of a liquid mixture diffuse through a selective membrane, evaporate under low pressure on the downstream side, and are removed by a vacuum pump or a chilled condenser [16]. Proper membrane materials are important to a PV process. For pervaporation removing organics from water, there are many kinds of materials that have been studied. For example, Takegami et al. [17] used PDMS membrane to separate ethanol/water mixtures; Liu et al. [18] used silicalite membrane to separate acetone solutions. In another report, ionic liquid-PDMS membrane was applied by Izák et al. in removing acetone from water [19]. Solak and Şanlı [20] separated acetone/water mixture with sodium alginate-poly (vinyl pyrrolidone) membrane. Sakaki et al. [21] prepared a silicalite membrane to separate 1-butanol, 2-propanol, ethanol, and acetone from dilute aqueous solutions by pervaporation. Among all membrane materials, PDMS is regarded as the interesting and promising one [22]. In order to improve membrane organophilic property, many studies on PDMS modifications have been delivered [23–31]. The modifications encompass filling [27,28], blending [25,31], coating [29,30], grafting [23,24,26], and so on. Among these methods, filling obtained attentions because of its simpleness in operation and low costing in energy consumption. Many kinds of materials have been used as fillings to improve the PV performance of PDMS membranes. Polytetrafluoroethylene (PTFE) is a super-hydrophobicity material, which possesses the advantages of excellent thermal stability, erosive resistance, no poisonous and, so on. It had been successfully used in the fabrication of PVDF-PTFE hollow fiber membrane for the desalination of sea water [32].

We have reported a literature about PDMS-PTFE membranes which were supported by polyethylene terephthalate (PET) non-woven fabrics to separate chloroform from aqueous solution [33]. It showed that the adding of PTFE particles in PDMS matrix enhanced the crystallinity, hydrophobicity, mechanical strength, and thermal stability of the PDMS membrane. Through examination, the membrane possessed striking advantages in flux and separation factor and showed excellent PV performance in the separation of

chloroform/water mixture. In this study, using PVDF as the support layer due to its good hydrophobic and chemical stability, we prepared a PTFE filled PDMS composite membrane for the pervaporation of acetone from its aqueous. The effects of operating conditions (including feed flow rate, feed temperature, and feed concentration) and PTFE content in PTFE-PDMS membrane on PV performance were systematically investigated and the membranes showed good performance for PV of an acetone/water mixture.

2. Materials and methods

2.1. Materials

PVDF (void fraction 72.5%, pore diameter 0.15 μm), as membrane support layer, was obtained from Changzhou Haoxin Insulation Material Co., Ltd, China. Polydimethylsiloxane (PDMS) (Silicone Rubber 107, M_w 5000), cross linking agent ethyl silicate, and curing agent dibutyltin dilaurate were purchased from Shanghai resin Company, China. PTFE particles (Dyneon TF-9207) were used as the additive and their structural parameters, such as the density of 2.165 g/cm^3, specific surface area of 17 m^2/g, active component of 100%, and primary particle size of 120 nm [33], were as listed elsewhere. Acetone and n-heptane were reagent grade and obtained from Shanghai Ruen Jie Chemical Reagent Company, China.

2.2. Preparation of PDMS composite membrane

The preparation of the unfilled PDMS and the PTFE filled PDMS flat sheet composite membranes was described in our previous work [33]. The unfilled PDMS flat sheet composite membrane was prepared as follows. The casting solution containing 17 wt.% PDMS was prepared by dissolving PDMS, crosslinker ethyl silicate, and curing agent dibutyltin dilaurate in n-heptane (the mass ratio of them was $m_{PDMS}:m_{ethyl\ silicate}:m_{dibutyltin\ dilaurate} = 10:1:0.5$) and was magnetic stirred of about 3 h. The casting solution was poured onto the surface of the PVDF base membrane and was dried in the sterile room at room temperature for 24 h to form the PDMS/PVDF membrane. To prepare the PTFE-PDMS membranes, different amounts of dried PTFE particles were dispersed in the previous PDMS casting solution under stirring for 3 h and the PTFE-PDMS composite membranes with different PTFE contents (0 wt.% PTFE-PDMS, 10 wt.% PTFE-PDMS, 20 wt.% PTFE-PDMS, 30 wt.% PTFE-PDMS, and 40 wt.% PTFE-PDMS, according to the PTFE content) were produced. Then, the unfilled and the PTFE filled PDMS flat membranes were used to

investigate the effects of the PTFE on membranes' physical characterization and also on PV performances. In addition, the unfilled and filled PDMS membranes without support layer were also prepared to investigate the influence of the physicochemical properties of the filled membranes.

2.3. SEM characterization of membrane

In order to investigate the dispersion and compatibility of PTFE in PDMS polymer matrix, surface and cross-section morphologies of different PDMS-PTFE/PVDF composite membranes were observed through the scanning electron microscope apparatus (SEM) (JEOL Model JSM-5600 LV, Japan). The membranes were firstly fractured in liquid nitrogen to prevent the deformation of the samples, sputtered with gold, and then the structure of top surface and cross section were observed.

2.4. Swelling study

40×40 mm pieces of dried 20 wt.% PDMS-PTFE composite membranes without support were weighted by a highly sensitive electronic balance (JA2204E, Yoke company Shanghai) with an accuracy of 0.0001 g and were immersed in acetone aqueous at 30°C for 48 h. Then, the membranes were taken out from the solutions and their weights were measured immediately after wiping off the liquid on the membrane surfaces by filter paper. The degree of swelling (DS) of the membrane was determined by:

$$DS = \frac{(M_\infty - M_0)}{M_0} \tag{1}$$

where M_∞ is the mass of the fully swollen membrane in acetone aqueous and M_0 is the dried membrane, respectively.

2.5. Solution and diffusion experiments

According to the solution-diffusion mechanism, which is used to describe the mass transport of components through membrane, pervaporation process contains sorption, diffusion, and evaporation in three steps [15,34]. In other words, the separation performance of a pervaporation membrane is the results of the common actions of both solubility selectivity and diffusion selectivity [35–37]. In this paper, the effects of feed temperature and PTFE content on sorption performance and diffusion performance of pure solvent were studied. To get the amount of pure solvent that dissolved in the membranes, the following weight measurement was conducted. Dry membrane sample of 40×40 mm was weighed using a microbalance (JA2204E, 0.0001 g, Yoke company Shanghai), then it was immersed into pure acetone solvent or deionized water at different temperatures. Taken out from the solvent, wiped with tissue paper to remove the surface solvent, the sample was weighed as quickly as possible, and then it was dipped back into the liquid. The experiment was repeated several times at an interval of certain time until the weight of the sample kept
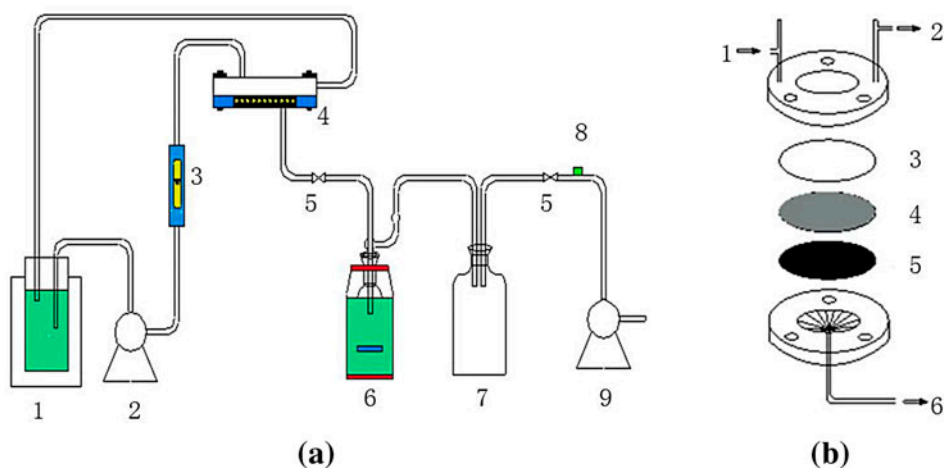

Fig. 1. (a) Schematic representation of PV separation of acetone–water mixtures: (1) feed tank; (2) peristaltic pump; (3) rotameter; (4) membrane module; (5) vacuum control valves; (6) cold trap; (7) surge flash; (8) vacuum indicator; (9) vacuum pump and (b) Schematic diagram of membrane module: (1) feed inlet; (2) retentate outlet; (3) O-ring; (4) membrane; (5) sintered disk; (6) permeate outlet.

approximately constant. The sorption coefficient (S) is defined by [38]:

$$S = (M'_\infty - M_0)/M_0 \qquad (2)$$

where M'_∞ is the mass of the fully swollen membrane in pure acetone or water solution.

The diffusion coefficients (D) of water and acetone in the membrane were measured from initial linear sorption curves [38–40]:

$$\frac{M_t}{M'_\infty} = \frac{4}{\pi^{1/2}} \sqrt{\frac{Dt}{L^2}} \qquad (3)$$

where M_t is the mass of the absorbed solvent in swollen membrane at time t. L is initial thickness of membrane. The diffusion coefficients of the water and acetone were obtained from the slopes of plots of M_t/M'_∞ vs. $t^{1/2}$ according to above equation.

According to the solution-diffusion mechanism, we defined ideal solubility selectivity α_s, ideal diffusion selectivity α_D, and ideal separation factor α_P as follows [41]:

$$\alpha_s = S_i/S_j \qquad (4)$$

$$\alpha_D = D_{i,\infty}/D_{j,\infty} \qquad (5)$$

$$\alpha_P = \alpha_S \alpha_D \qquad (6)$$

where i and j represent acetone and water, respectively.

2.6. Pervaporation

Pervaporation experiments were performed using a pervaporation laboratory rig schematically as shown in Fig. 1(a) and (b), which shows the schematic diagram of membrane module specifically. The pore size and porosity of sintered disk (Fig. 1(b)) were about 40 μm and 80%, respectively.

Membrane sample was placed in a cross-flow laboratory scale flat membrane unit. The effective area of membrane was 28.26 cm^2 and the capacity of the feed compartment was 10 L. The feed was circulated between membrane module and feed tank by a peristaltic pump. The downstream pressure of the membrane cell was maintained at 1.3 kPa by a vacuum pump. After the system reached a steady state (at least 2 h after starting), the permeate started to be collected in a cold trap which was immersed in liquid nitrogen.

Then, the permeate was analyzed by a gas chromatograph (GC-2014c, Shimadzu, Japan), which was equipped with a thermal conductivity detector (TCD) (the type of column was Porapak and the carrier gas was hydrogen (H_2)). The operating temperatures for the injector, detector, and oven were 250, 250, and 80°C, respectively.

The PV performance of membrane is usually expressed in terms of permeation flux J, separation factor α, and permeate separation index PSI as follows:

$$J = \Delta m/(A \cdot \Delta t) \qquad (7)$$

$$\alpha = (y_{acetone}/y_{water})/(x_{acetone}/x_{water}) \qquad (8)$$

$$PSI = (\alpha - 1) \cdot J \qquad (9)$$

where Δm is the weight of permeate, A is the effective area of the membrane, and Δt is the time interval of the permeation. x and y represent the mole fraction of a component in the feed and the permeate, respectively.

In some literatures [15,42], another approach to present pervaporation results was proposed. Permeance (P_i/L) and selectivity ($\beta_{i/j}$) were used to express the intrinsic properties of membranes without taking into account the experiment conditions and they are defined by:

$$\frac{P_i}{L} = \frac{J_i}{x_i \gamma_i p_i^{sat} - y_i p^p} \qquad (10)$$

where p^{sat} is the saturated vapor pressure of component. γ is the activity coefficient. p^p is the permeate pressure.

Further, the fugacity (f) of component i on feed side could be defined as [43]:

$$f_i = x_i \gamma_i p_i^{sat} \qquad (11)$$

Hence,

$$\frac{P_i}{L} = \frac{J_i}{(f_i - y_i p^p)} \qquad (12)$$

$$\beta_{i/j} = \frac{P_i/L}{P_j/L} = \frac{P_i}{P_j} \qquad (13)$$

The values of activity coefficient and saturated vapor pressure were calculated with Aspen Plus 7.3 and the non-random two liquid (NRTL) model was used.

3. Results and discussion

3.1. Membrane characterization

3.1.1. SEM studies

The surface and cross-section morphologies of the PTFE-PDMS/PVDF composite membranes containing different PTFE contents are presented in Fig. 2. The surface of the unfilled membrane was smooth and uniform. With the increasing in the PTFE content, the surfaces of the composite PTFE-PDMS membranes became rougher and rougher. According to literatures [1,44], the rough appearance of the filled membrane caused the increase in the effective contact area which in turn could result in an enhancement in flux. When the content of PTFE was 30 wt.%, the particle aggregation appeared. When the content of PTFE further increased to 40 wt.%, the surface was much rougher than that of the 30 wt.% one's: the PTFE particles aggregated evidently and the appreciable voids between PTFE and PDMS appeared, which also could be observed clearly from the cross-section (4,000×) picture of 40 wt.% PTFE-PDMS/PVDF membrane. The cross-section pictures of various composite membranes in Fig. 2 showed that the PTFE filled PDMS skin layers of about $10 \pm 1\ \mu m$ in thickness tightly adhered to the surfaces of the PVDF support layers.

3.1.2. Membrane swelling studies

The effects of acetone content on the swelling degree of the 20 wt.% PTFE-PDMS composite membrane were investigated. As shown in Fig. 3, the swelling degree of membrane was increased with the increasing acetone content in feed. This indicated that the membrane had good affinity for acetone.

3.1.3. Membrane solubility and diffusivity studies

In pervaporation, solubility and diffusivity of an individual component in the feed are important for the understanding of PV performance. Fig. 4 displays the typical sorption isotherms of pure acetone (a) and pure water (b) in PDMS and PTFE-PDMS composite membranes. Fig. 5 shows the typical sorption isotherms of pure acetone (a) and pure water (b) for the 20 wt.% PTFE-PDMS membrane at different feed temperatures. The uptake of water was far less than that of acetone for all membranes. It was shown that PDMS and PTFE-PDMS membranes had higher affinity to acetone than to water. In order to compare the interaction among acetone, water, and polymers, Hansen solubility parameter (HSP) which describes the cohesive energy between two molecules was introduced. It can be expressed by the following equation [45]:

$$\delta = \sqrt{\delta_d^2 + \delta_p^2 + \delta_h^2} \tag{14}$$

where δ is the Hansen solubility parameter for the component and δ_d, δ_p, δ_h refer to the dispersion solubility parameter, polar solubility parameter, and hydrogen bonding solubility parameter, respectively. From the definition of HSP, we can conclude that the more similar the HSPs of two components are, the higher their affinities will be. Table 1 shows the HSP data of PDMS, PTFE, acetone, and water. The affinities of both PDMS and PTFE toward acetone were higher than toward water. This was consistent with the adsorption test results.

From Fig. 6(a), the sorption coefficient of composite membranes in pure acetone solution decreased with the increase in PTFE content in membranes. The reason for this might be that the incorporation of PTFE into PDMS resulted in an increase in membrane crystallization and caused the increase in the rigidity of the filled membranes, as we reported in our previous work [33]. For the diffusion coefficients of acetone and water, both of them increased evidently with the increase in PTFE content in membrane. It might occur for the reason that PTFE interfered with the tight packing of PDMS chains [46], which made the diffusion of the permeating molecules through the filled membranes easier.

Fig. 6(b) shows the variations of the sorption coefficient and diffusion coefficient of the 20 wt.% PTFE-PDMS membrane in pure acetone and water at different temperatures. With the increase in temperature from 30 to 50°C, sorption coefficient of membrane in acetone increased from 0.249 to 0.296. It might be that during the dissolving process, the interactions of permeates, such as water–water, water–acetone and acetone–acetone, might have an enhancing effect on the energy required for the dissolution. In contrast, the interactions of permeates and the membrane were thought to diminish the energy required for dissolving. Therefore, the lower the temperature and the stronger the association of permeates are, the lower the sorption coefficient would be. As feed temperature increased, the interaction between two permeate molecules became weaker and the interaction between a permeate molecule and the membrane became stronger; so with the increase in feed temperature, solubility coefficient increased. Similarly, diffusion coefficients of both acetone and water also
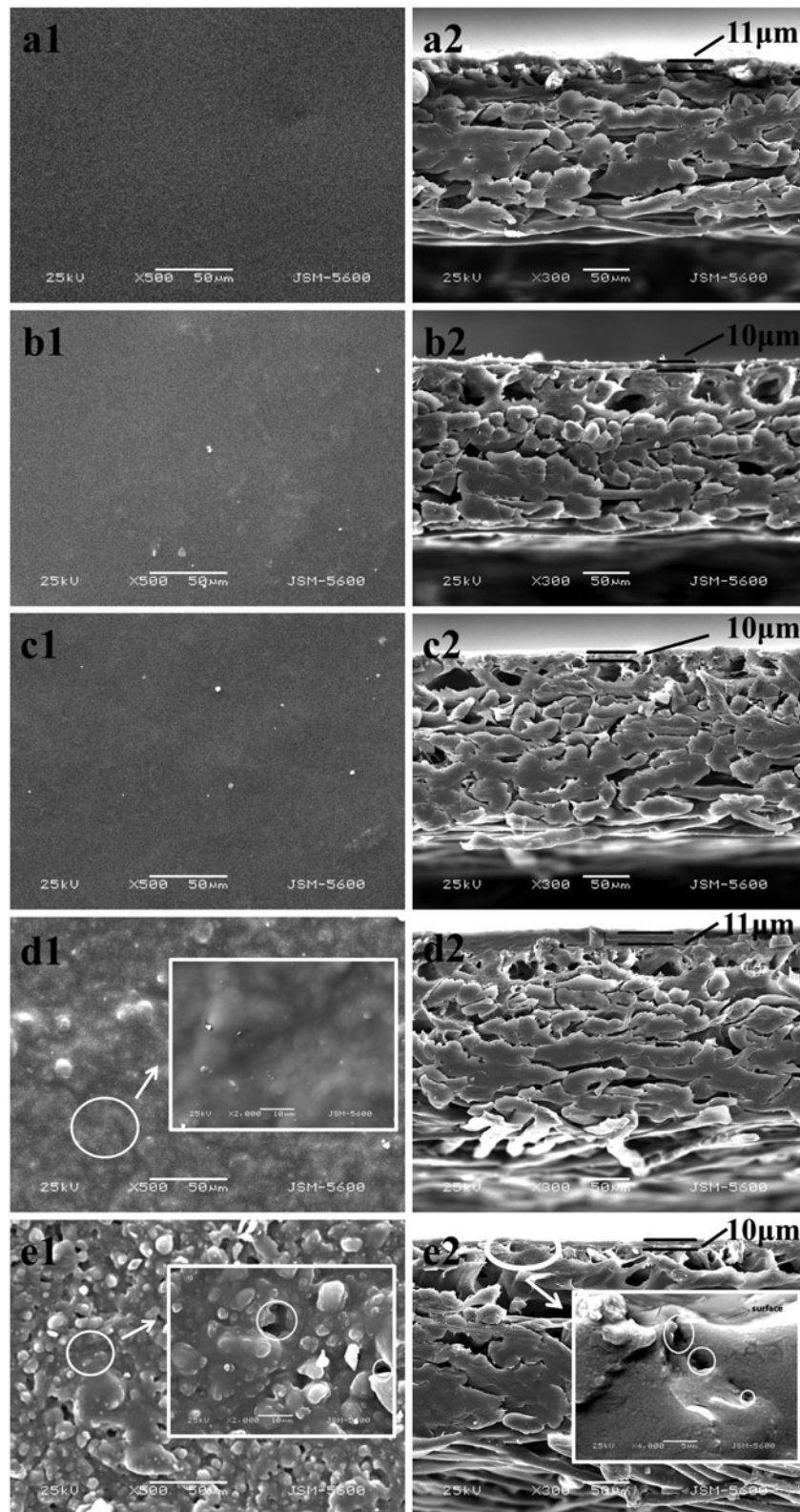
Fig. 2. SEM photographs of the PTFE-PDMS/PVDF composite membranes with different PTFE contents: (a–e) represent 0–40 wt.% PTFE-PDMS/PVDF composite membranes; (1) Top surface (500×) and (2) cross section (300×) of various composite membranes.
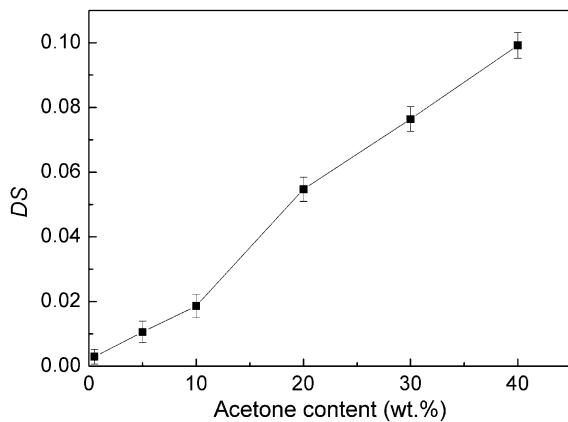
Fig. 3. Effect of acetone content on the swelling degree of 20 wt.% PTFE-PDMS composite membrane in various acetone aqueous.

increased obviously with the increasing feed temperature. This could be interpreted from two aspects. On the one hand, with the increase in feed temperature, the interaction of the permeate molecules as mentioned above became weaker which reduced the transfer resistance and stimulated the diffusions of the permeate molecules through the membrane [47]. On the other hand, it was well known that, the higher the temperature is, the greater the kinetic energy will be. So with the increase in feed temperature, the mobility of polymer chains increased and free volume of the matrix enhanced.

Fig. 7(a) shows the effects of PTFE content on solubility selectivity and diffusion selectivity of pure acetone and water at 30°C. With an increase in PTFE

content from 0 to 40 wt.%, solubility selectivity increased; diffusion selectivity firstly increased slightly and then decreased. This might be because that, with the increase in PTFE content, membranes hydrophobicity increased (the contact angle increased from 109.5° to 119.0° as studied from our previous work [33]), which caused the increase in solubility selectivity. However, when PTFE content exceeded 20 wt.%, according to the analysis of Section 3.1.1, on the surface of membrane, the particle aggregation and appreciable voids with no selectivity made the diffusion of permeates through the membrane easier. In addition, water molecule (0.3 nm) is much smaller than that of acetone one (0.47 nm) [15], so water can diffuse through membrane easier. As a result, diffusion selectivity decreased. The varying trends of solubility selectivity and diffusion selectivity made the ideal separation factor firstly increased and then decreased as shown in Fig. 7(b).

The effects of feed temperature on acetone solubility selectivity and diffusion selectivity were studied using the 20 wt.% PTFE-PDMS membrane as showed in Fig. 8(a). With the increase in feed temperature from 30 to 50°C, both solubility selectivity and diffusion selectivity of acetone decreased. Possible explanation could be that, firstly, with increasing feed temperature, water uptake increased more quickly than acetone (as seen from Fig. 5), which caused the decrease in solubility selectivity. Secondly, as we mentioned before, the increase in feed temperature would cause the increases in the mobility of the polymer chains and in the free volume of the matrix. Furthermore, high-feed temperature favored the diffusion of the small molecules of water over that of the large
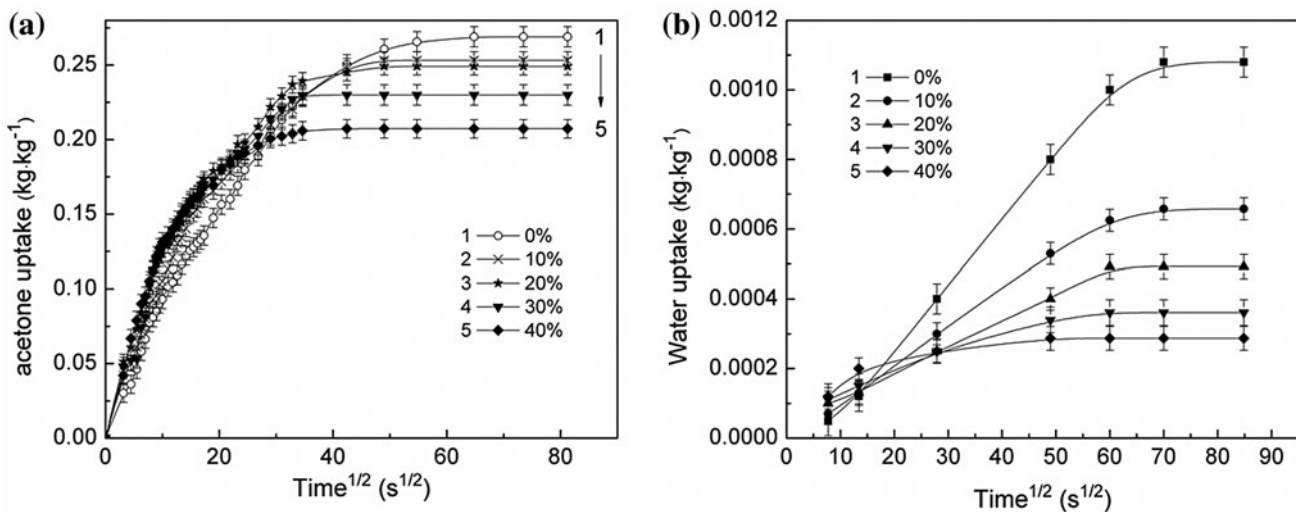

Fig. 4. Sorption isotherms of (a) pure acetone and (b) water in different PTFE-PDMS membranes at 30°C.
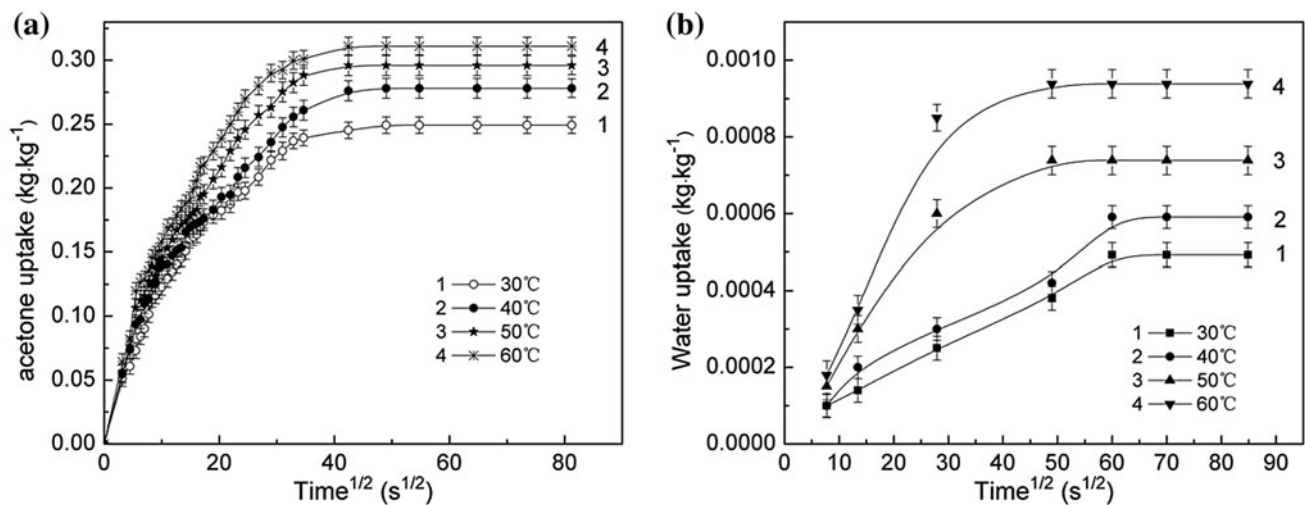
Fig. 5. Sorption isotherms of (a) pure acetone and (b) water in PTFE-PDMS membranes (PTFE: 20 wt.%) at different temperatures.

Table 1
Hansen solubility parameters of PDMS, PTFE, acetone, and water

Materials	δ_d [41]	δ_P [41]	δ_h [41]	δ
PDMS	15.9	0.10	4.7	16.6
PTFE	12.7	0.0	0.0	12.7
Acetone	15.5	10.4	7.0	19.9
Water	15.5	16.0	42.4	47.9

molecules of acetone [48]. So diffusion selectivity decreased. As a result, the ideal separation decreased with the increase in feed temperature as shown in Fig. 8(b).
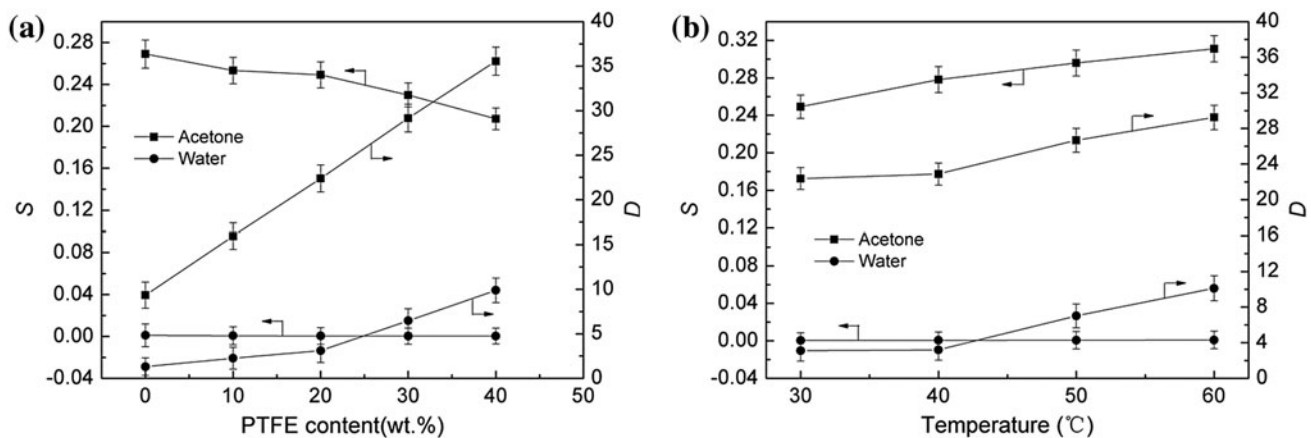
3.2. PV performance

3.2.1. Effect of PTFE content

The effects of PTFE content on partial flux and separation factor are shown in Fig. 9(a) (acetone concentration 30 wt.%, feed temperature 30°C, permeate-side vacuum 1.3 kPa, and feed flow rate 1,600 mL/min). Transport properties of water and acetone through PDMS-PTFE membranes depended strongly on PTFE content in the membrane. When there was no filling of PTFE, which means for the pure PDMS membrane, the fluxes of both water and acetone were the lowest. With an increase in PTFE adding, acetone and water fluxes increased correspondingly. When PTFE content was larger than 20 wt.%, the fluxes followed a rapid

Fig. 6. Effects of (a) PTFE content and (b) temperature on solubility coefficient and diffusion coefficient of acetone and water.
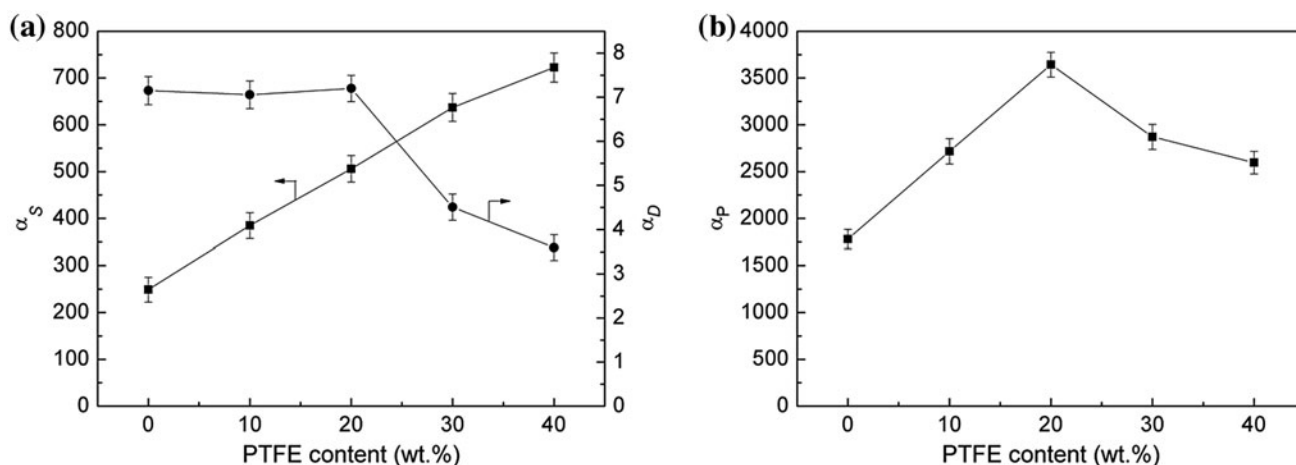
Fig. 7. Effects of PTFE content on (a) solubility selectivity, diffusion selectivity, and (b) ideal separation factor for pure acetone over water.
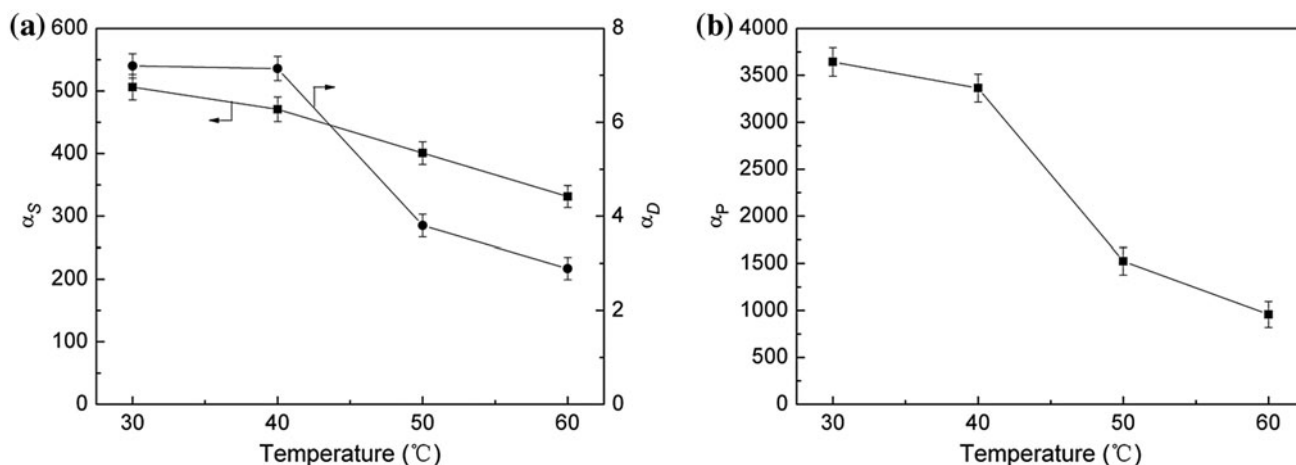

Fig. 8. Effects of operating temperature on (a) solubility selectivity, diffusion selectivity, and (b) ideal separation factor for pure acetone over water.

enhancement. Similar changing trend was also found by Kumar et al. [49], who studied the separation of n-hexane/acetone mixtures using the high density polyethylene (HDPE)/ethylene propylene diene terpolymer rubber (EPDM) blend polymer membranes by pervaporation.

Due to the higher affinity between an acetone molecule and the PTFE matrix, as analyzed in Section 3.1.3, acetone molecules could be preferentially adsorbed and diffused in the membrane (as shown in Fig. 6(a)) than water, which led to the increased acetone flux with the increase in PTFE content, and from Fig. 9(a), when PTFE content was 20 wt.%, acetone flux was 169 g/(m^2 h). We also found, with the increase in PTFE content, water flux increased too.

This could be that the agglomerate of the PTFE particles generated lots of interspaces among primary PTFE particles, which was beneficial to the diffusion of water molecules [31] (as shown in Fig. 6(a)). When PTFE content increased, separation factor increased to its maximum value 40 at 20 wt.% PTFE content and then decreased sharply. This is because, as analyzed for Fig. 2, particle aggregation appeared on the surface of the 30 wt.% PTFE membrane and when PTFE content reached 40 wt.%, appreciable voids emerged.

For the reason that separation factor and flux presented reversed changing trends when PTFE content exceeded 20 wt.%, we introduced PSI to evaluate the overall performance of the PTFE-PDMS membranes. Fig. 9(b) showed that the changing trend of PSI was
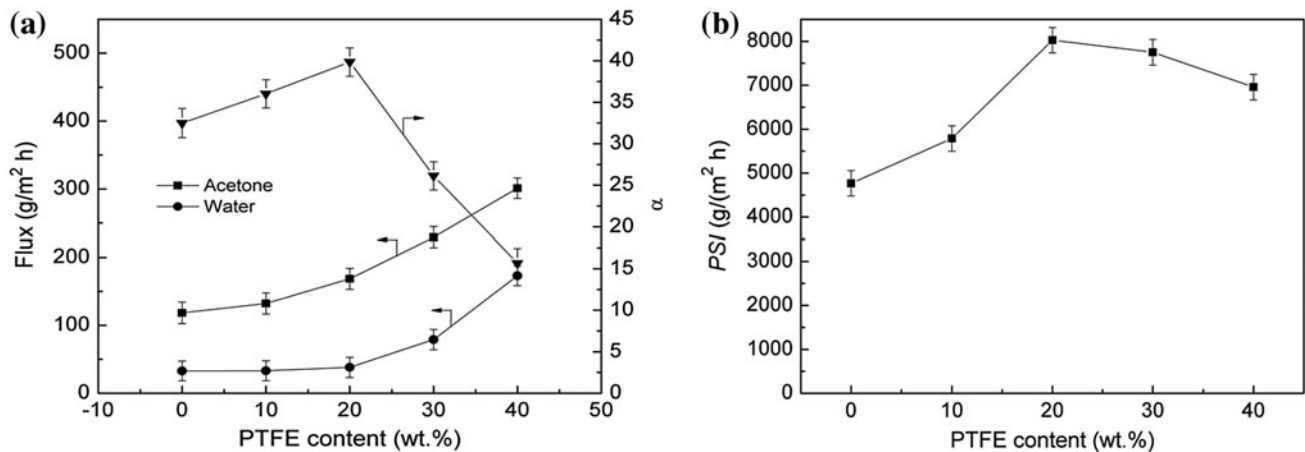
Fig. 9. Effects of PTFE content on (a) flux and separation factor and (b) PSI (Conditions: acetone concentration 30 wt.%, feed temperature 30 °C, permeate-side vacuum 1.3 kPa, and feed flow rate 1,600 mL/min).

similar to that of the separation factor. When PTFE filling was 20 wt.%, PSI reached its maximum value 8,015 g/(m² h), a 168.3% improvement compared with the unfilled PDMS membrane which was 4,769 g/(m² h). So we could conclude that the 20 wt.% PTFE filled membrane had the best pervaporation properties for the separation of acetone aqueous solution.

3.2.2. Effect of feed temperature

The effects of operating temperature on partial per-meation flux and separation factor for the 30 wt.% ace-tone solution at 1.3 kPa vacuum and 1,600 mL/min feed flow rate are illustrated in Fig. 10. The increase in feed temperature resulted in the slight increase in fluxes of acetone and water for the 20 wt.% PTFE-PDMS membrane. The reason is that the increasing feed temperature weakened the interactions among the permeate molecules (as analyzed in Section 3.1.3) and caused the increase in driving force, which promoted the dissolution and diffusion of permeate molecules (as shown in Fig. 6(b)). Therefore, as shown in Fig. 10, with the increase in feed temperature, partial fluxes of both water and acetone increased. Similar results were reported by Khayet, et al. [13], who investigated the separation of acetone solution by membrane Pervap 4060. They reported that with the increase in feed temperature, feed vapor pressure increased exponentially, so overall mass transfer coefficient increased, consequently permeate flux increased. However, with the increase in feed temper-ature, acetone solubility selectivity and diffusion selec-tivity decreased, as showed in Fig. 8(a), and caused
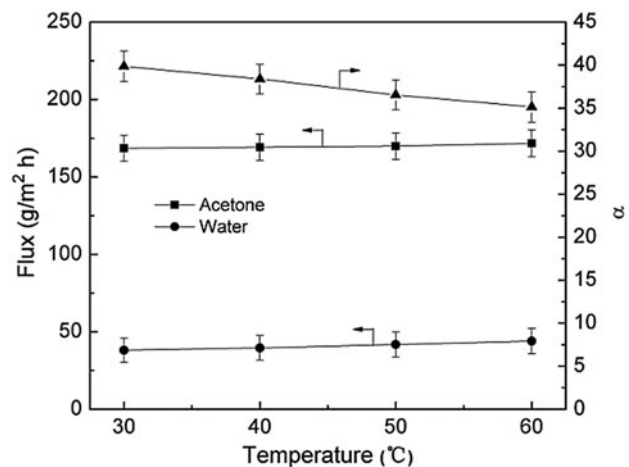

Fig. 10. Effect of temperature on flux and separation factor (Conditions: PTFE content 20 wt.%, acetone concentration 30 wt.%, permeate-side vacuum 1.3 kPa, and feed flow rate 1,600 mL/min).

the slight decrease in the separation factor, which was in close agreement with the changing trend of ideal separation factor (Fig. 8(b)).

Generally, from the view of thermodynamics, the effects of feed temperature on permeate flux can be described by Arrhenius equation which was reported frequently in pervaportion processes [15,50–53]:

$$J = J_0 \exp\left(-\frac{E_a}{RT}\right) \tag{15}$$

where J_0 is pre-exponential factor, J is permeate flux, E_a is the apparent activation energy, which includes

the activation energy for permeability and the heat of vaporization. R is gas constant and T is absolute feed temperature. In order to determine the E_a of each component, a semi-logarithmic plot of permeation flux against reciprocal of absolute temperature $(1/T)$ was developed, as shown in Fig. 11. The calculated apparent activity energy values for acetone and water were 0.504 and 4.08 kJ/mol, respectively. A higher value of the E_a implies a more sensitive behavior toward temperature alteration [54]. For the reason that the E_a of water was bigger than that of the acetone, water flux was more dependent on the changing of feed temperature [55], which resulted in the separation factor of acetone decreased with the increasing in feed temperature.

3.2.3. Effect of feed flow rate

Fig. 12 presents the effects of feed flow rate on partial flux and separation factor for the 20 wt.% PTFE-PDMS composite membrane at 30℃ and 1.3 kPa for the separation of the 30 wt.% acetone solution. Date in Fig. 12 indicates that when feed flow rate increased from 60 to 2,000 mL/min, flux firstly increased and then kept an asymptotic value when feed flow rate exceeded 900 mL/min, where the separation factor reached its maximum value of 40 and then kept constant.

It is well known that concentration polarization has an important influence on the penetration of VOCs through the composite membrane in pervaporation process [56,57]. Due to the PTFE-PDMS membranes are much more permeable to acetone than to

Fig. 12. Effects of feed flow rate on flux and separation factor.
Notes: Conditions: PTFE content 20 wt.%, feed temperature 30℃, acetone concentration 30 wt.%, and permeate-side vacuum 1.3 kPa.

water, the layer of acetone aqueous immediately adjacent to the membrane surface becomes depleted and the concentration polarization occurred accordingly. According to Baker and Wijmans's studies for concentration polarization [57], the turbulence, which determined by the feed flow rate through a membrane module, has an effect on controlling the concentration polarization and the minimum effective fluid velocity could be determined by the curve of fluid velocity and separation factor. From Fig. 12, when the feed flow rate is less than 900 mL/min, partial fluxes and separation factor increased with the increase in feed flow rate. This might be due to the increased feed flow rate that decreased the thickness of stagnant boundary layer next to the membrane and then decreased the permeation resistance of components. With the further increase in feed flow rate, acetone flux, water flux, and separation factor tend to be constant, which might be the result of the disappearance of the stagnant boundary layer. And the velocity of 900 mL/min is the minimum effective fluid velocity to control the effect of concentration polarization.

3.2.4. Effect of feed concentration

Fig. 13 shows the effects of feed concentration (0.5–30 wt.%) on acetone flux, water flux, and separation factor at 30℃, 1.3 kPa, and 1,600 mL/min for the 20 wt.% PTFE-PDMS membrane. With the increasing in feed concentration, acetone flux and separation factor increased obviously; water flux remained constant and was far less than acetone flux. The increase in
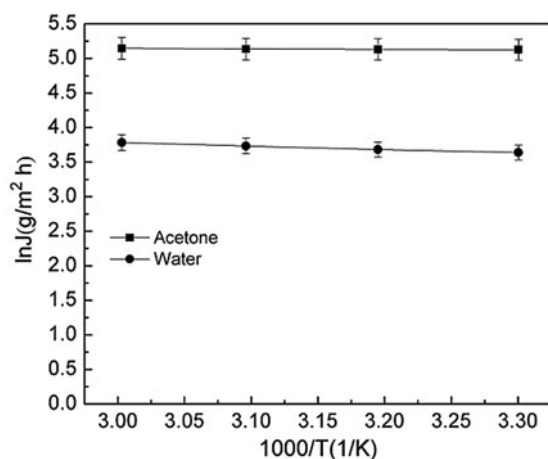

Fig. 11. Arrhenius plot of $\ln J$ vs. $1/T$ (Conditions: PTFE content 20 wt.%, acetone concentration 30 wt.%, permeate-side vacuum 1.3 kPa, and feed flow rate 1,600 mL/min).
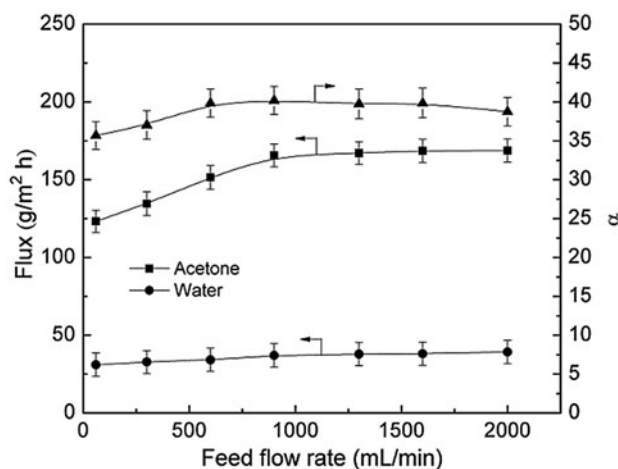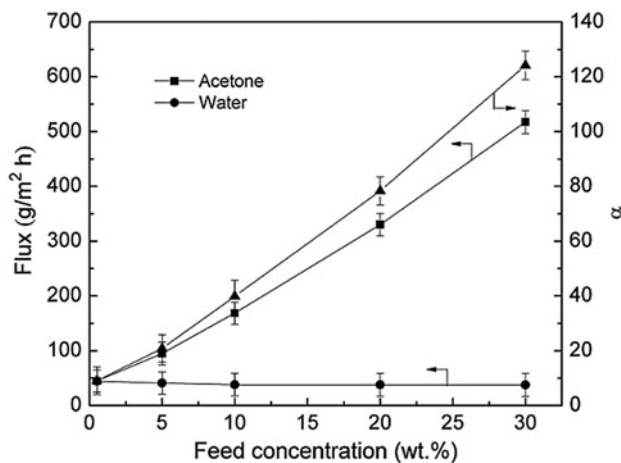
Fig. 13. Effects of feed concentration on acetone flux, water flux, and separation factor.
Notes: Conditions: PTFE content 20 wt.%, feed temperature 30℃, permeate-side vacuum 1.3 kPa, and feed flow rate 1,600 mL/min.
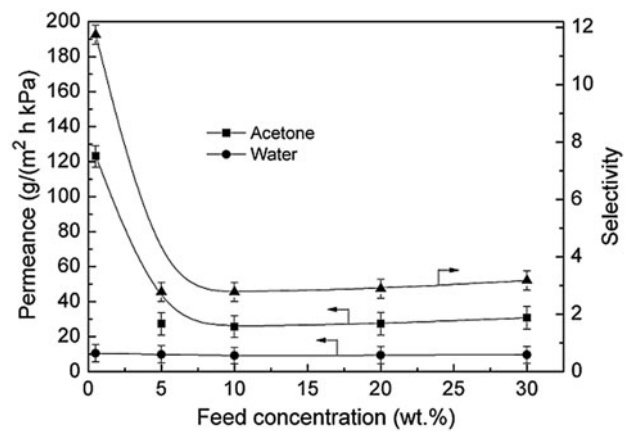

Fig. 14. Effect of feed concentration on the acetone and water permeance and intrinsic selectivity of 20 wt.% PTFE-PDMS composite membrane.
Notes: Conditions: feed temperature 30℃, permeate-side pressure 1.3 kPa, and feed flow rate 1600 mL/min.

acetone flux might be due to the increase in acetone vapor partial pressure, which caused the increase in the driving force for acetone to penetrate the membrane. Theoretically, with the decrease in water content in feed, the vapor partial pressure of water should decrease, which should in turn cause the decrease in the water flux. However, in this study, water flux remained constant. This could attribute to the swelling of membrane in acetone aqueous as analyzed in Section 3.1.2. With the increasing in acetone content in feed, the swelling degree of composite membrane increased, which benefits the penetration of water through the membrane [27,33]. As a result, with the change of feed concentration, there was not a big change in water flux. The swelling of the membrane could also promote the permeation of acetone in membrane, accordingly, with the increasing in acetone content in feed, acetone flux increased obviously. The changes of acetone flux and water flux resulted in the change of separation factor which increased with the increasing in feed concentration according to Eq. (8).

In order to study the effects of feed concentration on membrane intrinsic properties, Fig. 14 displays the relationships of permeance and selectivity to feed concentration. With the increase in acetone content from 0.5 to 10 wt.%, acetone permeance and selectivity decreased sharply, but with the further increase in feed concentration, acetone permeance and selectivity remained to a plateau value. In addition, water permeance kept constant in the studied concentration range. The reduced acetone permeance and selectivity might be explained by Baker's crowding (saturation) effect

[42]: with the increase in feed concentration, the adsorption of acetone on composite membrane would gradually get close to the saturation, which could lead to the increment of acetone content slowdown in membrane. The similar result was reported by Zhou et al. [58], who used PDMS/PVDF composite membrane to separate dimethyl carbonate from a methanol solution. According to the definition of permeance (Eq. (12)), the constant water permeance could attribute to the marginal change of water flux (Fig. 13) and water fugacity (Fig. 15) with the change of feed concentration. Similar phenomenon was reported
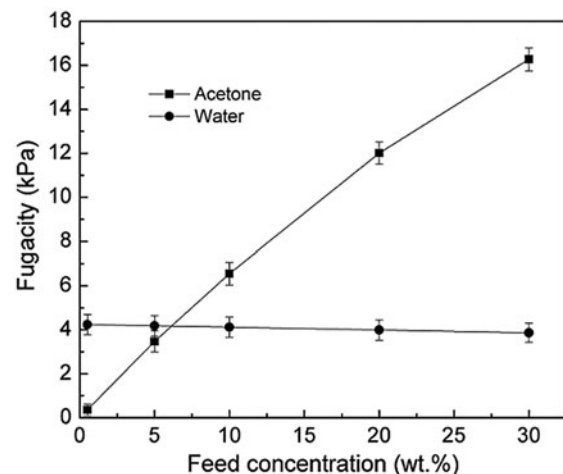

Fig. 15. Effects of feed concentration on fugacity of acetone and water.
Notes: Conditions: feed temperature 30℃, permeate-side pressure 1.3 kPa.

elsewhere for other organic-water mixtures [43,59]. The permeance changes of acetone and water resulted in selectivity decreased in line with Eq. (13).

4. Conclusion

A composite membrane with the PTFE filled PDMS as the top active layer and PVDF membrane as the support layer was prepared for the pervaporation of acetone/water aqueous solution. Membrane SEM graphs showed that the surfaces of the PTFE-PDMS membranes became rougher and rougher with the increasing PTFE content. When the PTFE content was 30 wt.%, the particle aggregation appeared; when the content of PTFE reached 40 wt.%, the particle aggregated more evidently and appreciable voids between PTFE and PDMS appeared. According to the cross-section pictures of various PDMS-PTFE/PVDF membranes, the PTFE filled PDMS skin layers were about 10 ± 1 μm.

Due to the good affinity between membrane and acetone, the swelling degree of 20 wt.% PTFE-PDMS membrane was increased with the increasing acetone concentration in feed. In addition, this good affinity also made the uptake of the water less than the uptake of the acetone according to membrane solubility and diffusivity studies. With an increase in PTFE content from 0 to 40 wt.%, membrane crystallization increased and the tight packing of PDMS chains was interfered, which led to the solubility selectivity increased and diffusion selectivity firstly increased and then decreased. When the temperature increased from 30 to 50℃, solubility selectivity, diffusion selectivity, and ideal separation factor had the same trends in which they decreased for the reasons of the increased interaction between the acetone and the membrane and the decreased transfer resistance of the permeate.

Incorporating PTFE into PDMS membrane could significantly influence the PV properties of the membranes for the 30 wt.% acetone aqueous. With an increase in PTFE content from 0 to 40 wt.%, acetone flux increased accordingly. This was because the HSP of acetone and polymer matrix were very similar, so acetone could be preferentially adsorbed and diffused in membrane. However, due to the particle aggregation appeared when PTFE content exceed 20 wt.%, separation factor reached its maximum when PTFE content was 20 wt.%. For the influence of feed temperature, fluxes of acetone and water increased and separation factor decreased slightly with the increase in feed temperature for the tested 20 wt.% PTFE-PDMS composite membrane when feed concentration was 30 wt.% and the permeate-side vacuum was 1.3 kPa.

The effects of feed temperature on permeate flux followed the Arrhenius relationship and the apparent activation energy calculated from the slope were 0.50 and 4.08 kJ/mol for acetone and water, respectively. With the increase in feed flow rate from 60 to 2,000 mL/min, acetone flux and separation factor increased at the beginning and then tended to be constant which attributed to the effects of the increased turbulence on the concentration polarization. Feed concentration also influenced the permeation performance, when feed concentration increased from 0.5 to 30 wt.%, acetone flux and separation factor increased, while water flux remained stable. Moreover, the crowding effect made the permeance of acetone and selectivity decreased firstly and then maintained a plateau value. The small changes in water flux and fugacity resulted in a constant water permeance.

List of symbols

S		sorption coefficient
M_0	—	mass of dried membrane (g)
$M_{i,\infty}$	—	mass of wet membrane at solution equilibrium (g)
M_t	—	the mass of the absorbed solvent in swollen membrane at time t (g)
D	—	diffusion coefficient
$D_{i,\infty}$	—	diffusion coefficient of component i in membrane at solution equilibrium
α_s	—	ideal solubility selectivity
α_D	—	ideal diffusion selectivity
α_P	—	ideal separation factor
t	—	time in min
L	—	thickness of membrane (μm)
J	—	permeate flux (g/(m^2 h))
m	—	weight of permeate (g)
A	—	effective area of membrane (m^2)
Δt	—	time interval of the permeation (h)
α	—	separation factor
x	—	mole fraction of a component in the feed
y	—	mole fraction of a component in the permeate
PSI	—	permeate separation index (g/(m^2 h))
δ	—	Hansen solubility parameter of component
δ_d	—	dispersion solubility parameter
δ_P	—	polar solubility parameter
δ_h	—	hydrogen bonding solubility parameter

J_0 — pre-exponential factor
E_a — the apparent activation energy (kJ/mol)
R — universal gas constant (J/mol K)
T — absolute feed temperature (K)
P/L — permeance (g/(m^2 h kPa))
f — fugacity, (kPa)
β — selectivity
p^{sat} — saturated vapor pressure (kPa)
γ — activity coefficient
p^P — permeate pressure (kPa)

Subscript
i, j   — component i, j

References

[1] J. Li, G.J. Zhang, S.L. Ji, N.X. Wang, W. An, Layer-by-layer assembled nanohybrid multilayer membranes for pervaporation dehydration of acetone–water mixtures, J. Membr. Sci. 415–416 (2012) 745–757.

[2] S. Gagne, K. Volchek, D. Velicogna, R.K. Tyagi, T. Matsuura, Removal of acetone from oily waste water by pervaporation, in: R. Bakish (Ed.), Proc. Sixth Int. Conf. Pervaporation Processes Chem. Ind, Bakish Materials Corp., (1992), 411.

[3] W.L. Luyben, Pressure-swing distillation for minimum- and maximum-boiling homogeneous azeotropes, Ind. Eng. Chem. Res. 51 (2012) 10881–10886.

[4] T.J. Levario, M.Z. Dai, W. Yuan, B.D. Vogt, D.R. Nielsen, Rapid adsorption of alcohol biofuels by high surface area mesoporous carbons, Microporous Mesoporous Mater. 148 (2012) 107–114.

[5] X. Lin, J. Wu, J. Fan, W. Qian, X. Zhou, C. Qian, X. Jin, L. Wang, J. Bai, H. Ying, Adsorption of butanol from aqueous solution onto a new type of macroporous adsorption resin: Studies of adsorption isotherms and kinetics simulation, J. Chem. Technol. Biotechnol. 87 (2012) 924–931.

[6] P.L. Edmiston, L.A. Underwood, Absorption of dissolved organic species from water using organically modified silica that swells, Sep. Purif. Technol. 66 (2009) 532–540.

[7] T.C. Ezeji, N. Qureshi, H.P. Blaschek, Bioproduction of butanol from biomass: From genes to bioreactors, Curr. Opin. Biotechnol. 18 (2007) 220–227.

[8] D. Cai, Z. Chang, L.L. Gao, C.J. Chen, Y.P. Niu, P.Y. Qin, Z. Wang, T.W. Tan, Acetone–butanol–ethanol (ABE) fermentation integrated with simplified gas stripping using sweet sorghum bagasse as immobilized carrier, Chem. Eng. J. 277 (2015) 176–185.

[9] R. Shukla, W. Kang, K.K. Sirkar, Acetone-butanol-ethanol (ABE) production in a novel hollow fiber fermentor-extractor, Biotechnol. Bioeng. 34 (1989) 1158–1166.

[10] F.A. Banat, M. Al-Shannag, Recovery of dilute acetone-butanol-ethanol (ABE) solvents from aqueous solutions via membrane distillation, Bioprocess Eng. 23 (2000) 643–649.

[11] I.L. Borisov, V.V. Volkov, V.A. Kirsh, V.I. Roldugin, Simulation of the temperature-driven pervaporation of dilute 1-butanol aqueous mixtures through a PTMSP membrane in a cross-flow module, Pet. Chem. 51 (2011) 542–554.

[12] A. Kujawska, J. Kujawski, M. Bryjak, W. Kujawski, Removal of volatile organic compounds from aqueous solutions applying thermally driven membrane processes. 1. Thermopervaporation, Chem. Eng. Process. Process Intensif. 94 (2015) 62–71.

[13] M. Khayet, C. Cojocaru, G. Zakrzewska-Trznadel, Studies on pervaporation separation of acetone, acetonitrile and ethanol from aqueous solutions, Sep. Purif. Technol. 63 (2008) 303–310.

[14] H.S. Samanta, S.K. Ray, Pervaporative recovery of acetone from water using mixed matrix blend membranes, Sep. Purif. Technol. 143 (2015) 52–63.

[15] A. Rozicka, J. Niemistö, R.L. Keiski, W. Kujawski, Apparent and intrinsic properties of commercial PDMS based membranes in pervaporative removal of acetone, butanol and ethanol from binary aqueous mixtures, J. Membr. Sci. 453 (2014) 108–118.

[16] W.L. McCabe, J.C. Smith, P. Harriott, Unit Operation of Chemical Engineering, sixth ed., McGraw-Hill, Chemical Industry Press Publication, New York, 2003, 883.

[17] S. Takegami, H. Yamada, S. Tsujii, Pervaporation of ethanol/water mixtures using novel hydrophobic membranes containing polydimethylsiloxane, J. Membr. Sci. 75 (1992) 93–105.

[18] Q. Liu, R.D. Noble, J.L. Falconer, H.H. Funke, Organics/water separation by pervaporation with a zeolite membrane, J. Membr. Sci. 117 (1996) 163–174.

[19] P. Izák, W. Ruth, Z. Fei, P.J. Dyson, U. Kragl, Selective removal of acetone and butan-1-ol from water with supported ionic liquid-polydimethylsiloxane membrane by pervaporation, Chem. Eng. J. 139 (2008) 318–321.

[20] E.K. Solak, O. Şanlı, Use of sodium alginate-poly(vinyl pyrrolidone) membranes for pervaporation separation of acetone/water mixtures, Sep. Sci. Technol. 45 (2010) 1354–1362.

[21] K. Sakaki, H. Habe, H. Negishi, T. Ikegami, Pervaporation of aqueous dilute 1-butanol, 2-propanol, ethanol and acetone using a tubular silicalite membrane, Desalin. Water Treat. 34 (2011) 290–294.

[22] C.K. Yeom, H.K. Kim, J.W. Rhim, Removal of trace VOCs from water through PDMS membranes and analysis of their permeation behaviors, J. Appl. Polym. Sci. 73 (1999) 601–611.

[23] T. Ohshima, Y. Kogami, T. Miyata, T. Uragami, Pervaporation characteristics of cross-linked poly(dimethylsiloxane) membranes for removal of various volatile organic compounds from water, J. Membr. Sci. 260 (2005) 156–163.

[24] T. Uragami, H. Yamada, T. Miyata, Removal of dilute volatile organic compounds in water through graft copolymer membranes consisting of poly(alkylmethacrylate) and poly(dimethylsiloxane) by pervaporation and their membrane morphology, J. Membr. Sci. 187 (2001) 255–269.

[25] S.J. Lue, T.H. Yang, K.S. Chang, K.L. Tung, Water diffusivity suppression and ethanol-over-water diffusion selectivity enhancement for ethanol/water mixtures in polydimethylsiloxane–zeolite membranes, J. Membr. Sci. 415–416 (2012) 635–643.

[26] W.W.Y. Lau, J. Finlayson, J.M. Dickson, J. Jiang, M.A. Brook, Pervaporation performance of oligosilylstyrene-polydimethylsiloxane membrane for separation of organics from water, J. Membr. Sci. 134 (1997) 209–217.

[27] Y. Shirazi, A. Ghadimi, T. Mohammadi, Recovery of alcohols from water using polydimethylsiloxane–silica nanocomposite membranes: Characterization and pervaporation performance, J. Appl. Polym. Sci. 124 (2012) 2871–2882.

[28] X.L. Liu, Y.S. Li, Y. Liu, G.Q. Zhu, J. Liu, W.S. Yang, Capillary supported ultrathin homogeneous silicalite-poly(dimethylsiloxane) nanocomposite membrane for bio-butanol recovery, J. Membr. Sci. 369 (2011) 228–232.

[29] G.P. Liu, W. Wei, W.Q. Jin, N.P. Xu, Ball milling 2,4,6-trichlorophenol with calcium oxide: Dechlorination experiment and mechanism considerations, Chem. Eng. J. 195–196 (2012) 62–68.

[30] H.J. Lee, E.J. Cho, Y.G. Kim, I.S. Choi, H.J. Bae, Pervaporative separation of bioethanol using a poly-dimethylsiloxane/polyetherimide composite hollow-fiber membrane, Bioresour. Technol. 109 (2012) 110–115.

[31] H.L. Zhou, Y. Su, X.R. Chen, Y.H. Wan, Separation of acetone, butanol and ethanol (ABE) from dilute aque-ous solutions by silicalite-1/PDMS hybrid pervapora-tion membranes, Sep. Purif. Technol. 79 (2011) 375–384.

[32] M.M. Teoh, T.S. Chung, Membrane distillation with hydrophobic macrovoid-free PVDF–PTFE hollow fiber membranes, Sep. Purif. Technol. 66 (2009) 229–236.

[33] D. Sun, B.B. Li, Z.L. Xu, Preparation and characteriza-tion of poly(dimethylsiloxane)-polytetrafluoroethylene (PDMS-PTFE) composite membrane for pervaporation of chloroform from aqueous solution, Korean J. Chem. Eng. 30 (2013) 2059–2067.

[34] Y.M. Lee, D. Bourgeois, G. Belfort, Sorption, diffusion, and pervaporation of organics in polymer membranes, J. Membr. Sci. 44 (1989) 161–181.

[35] G.M. Shi, H.M. Chen, Y.C. Jean, T.S. Chung, Sorption, swelling, and free volume of polybenzimidazole (PBI) and PBI/zeolitic imidazolate framework (ZIF-8) nano-composite membranes for pervaporation, Polymer 54 (2013) 774–783.

[36] A.M. Sajjan, B.K. Jeevan Kumar, A.A. Kittur, M.Y. Kariduraganavar, Novel approach for the develop-ment of pervaporation membranes using sodium algi-nate and chitosan-wrapped multiwalled carbon nanotubes for the dehydration of isopropanol, J. Membr. Sci. 425–426 (2013) 77–88.

[37] J.H. Chen, J.Z. Zheng, Q.L. Liu, H.X. Guo, W. Weng, S.X. Li, Pervaporation dehydration of acetic acid using polyelectrolytes complex (PEC)/11-phosphotungstic acid hydrate (PW$_{11}$) hybrid membrane (PEC/PW$_{11}$), J. Membr. Sci. 429 (2013) 206–213.

[38] H.M. Qu, Y. Kong, H.L. Lv, Y.Z. Zhang, J.R. Yang, D.Q. Shi, Effect of crosslinking on sorption, diffusion and pervaporation of gasoline components in hydrox-yethyl cellulose membranes, Chem. Eng. J. 157 (2010) 60–66.

[39] S. Das, A.K. Banthia, B. Adhikari, Removal of chlori-nated volatile organic contaminants from water by pervaporation using a novel polyurethane urea-poly (methyl methacrylate) interpenetrating network mem-brane, Chem. Eng. Sci. 61 (2006) 6454–6467.

[40] M. Mulder, Basic Principles of Membrane Technology, Kluwer Academic Publishers, Netherlands, 1996, 245.

[41] G.L. Han, Q.G. Zhang, Q.L. Liu, Separation of metha-nol/methyl tert-butyl ether using sulfonated pol-yarylethersulfone with cardo (SPES-C) membranes, J. Membr. Sci. 430 (2013) 180–187.

[42] R.W. Baker, J.G. Wijmans, Y. Huang, Permeability, permeance and selectivity: A preferred way of report-ing pervaporation performance data, J. Membr. Sci. 348 (2010) 346–352.

[43] H.S. Samanta, S.K. Ray, P. Das, N.R. Singha, Separation of acid–water mixtures by pervaporation using nanoparticle filled mixed matrix copolymer membranes, J. Chem. Technol. Biotechnol. 87 (2012) 608–622.

[44] W.C. Chao, S.H. Huang, Q.F. An, D.J. Liaw, Y.C. Huang, K.R. Lee, J.Y. Lai, Novel interfacially-polymer-ized polyamide thin-film composite membranes: Stud-ies on characterization, pervaporation, and positron annihilation spectroscopy, Polymer 52 (2011) 2414–2421.

[45] R.H. Perry, Chemical Engineer's Handbook, McGraw-Hill, New York, NY, 2001.

[46] Y. Nagase, T. Ando, C.M. Yun, Syntheses of siloxane-grafted aromatic polymers and the application to per-vaporation membrane, React. Funct. Polym. 67 (2007) 1252–1263.

[47] Q. Zhao, J.W. Qian, Q.F. An, Z.H. Zhu, P. Zhang, Y.X. Bai, Studies on pervaporation characteristics of poly-acrylonitrile-*b*-poly(ethylene glycol)-*b*-polyacrylonitrile block copolymer membrane for dehydration of aqueous acetone solutions, J. Membr. Sci. 311 (2008) 284–293.

[48] Y.J. Fu, C.L. Lai, J.T. Chen, C.T. Liu, S.H. Huang, W.S. Hung, C.C. Hu, K.R. Lee, Hydrophobic composite membranes for separating of water-alcohol mixture by pervaporation at high temperature, Chem. Eng. Sci. 111 (2014) 203–210.

[49] P.V.A. Kumar, S. Anilkumar, K.T. Varughese, S. Thomas, Separation of n-hexane/acetone mixtures by pervaporation using high density polyethylene/ethy-lene propylene diene terpolymer rubber blend mem-branes, J. Hazard. Mater. 199–200 (2012) 336–342.

[50] S. Chovau, S. Gaykawad, A.J.J. Straathof, B. Van der Bruggen, Influence of fermentation by-products on the purification of ethanol from water using pervapora-tion, Bioresour. Technol. 102 (2011) 1669–1674.

[51] B. Bettens, J. Degrève, B. Van der Bruggen, C. Vandecasteele, Transport of binary mixtures in perva-poration through a microporous silica membrane: Shortcomings of Fickian models, Sep. Sci. Technol. 42 (2007) 1–23.

[52] L. Aouinti, M. Belbachir, A maghnite-clay-H/ polymer membrane for separation of ethanol–water azeotrope, Appl. Clay Sci. 39 (2008) 78–85.

[53] Q.W. Yeang, S.H.S. Zein, A.B. Sulong, S.H. Tan, Comparison of the pervaporation performance of vari-ous types of carbon nanotube-based nanocomposites in the dehydration of acetone, Sep. Purif. Technol. 107 (2013) 252–263.

[54] V. García, E. Pongrácz, E. Muurinen, R.L. Keiski, Per-vaporation of dichloromethane from multicomponent aqueous systems containing *n*-butanol and sodium chloride, J. Membr. Sci. 326 (2009) 92–102.

[55] G.P. Liu, D. Hou, W. Wei, F.J. Xiangli, W.Q. Jin, Per-vaporation separation of butanol-water mixtures using

polydimethylsiloxane/ceramic composite membrane, Chin. J. Chem. Eng. 19 (2011) 40–44.

[56] J.G. Wijmans, A.L. Athayde, R. Daniels, J.H. Ly, H.D. Kamaruddin, I. Pinnau, The role of boundary layers in the removal of volatile organic compounds from water by pervaporation, J. Membr. Sci. 109 (1996) 135.

[57] R.W. Baker, J.G. Wijmans, A.L. Athayde, R. Daniels, J.H. Ly, M. Le, The effect of concentration polarization on the separation of volatile organic compounds from

water by pervaporation, J. Membr. Sci. 137 (1997) 159–172.

[58] H.L. Zhou, L. Lv, G.P. Liu, W.Q. Jin, W.H. Xing, PDMS/PVDF composite pervaporation membrane for the separation of dimethyl carbonate from a methanol solution, J. Membr. Sci. 471 (2014) 47–55.

[59] S.B. Kuila, S.K. Ray, Dehydration of acetic acid by pervaporation using filled IPN membranes, Sep. Purif. Technol. 81 (2011) 295–306.